Properties of the $\Lambda(1405)$ Hyperon Measured at CLAS

Kei Moriya
with
Reinhard Schumacher

Carnegie Mellon University

September 15, 2009

Outline

1. Introduction
   - motivation for the study of the $\Lambda(1405)$ – what is it?
   - theory of the $\Lambda(1405)$
   - goals of this analysis
2. CLAS Analysis
   - the g11a data set in CLAS at Jlab
   - cuts to the data
   - background
   - fits to the lineshape
3. Results
   - lineshape
   - cross section
   - spin-parity
4. Conclusion

what is the $\Lambda(1405)$?

- **** resonance just below $N\overline{K}$ threshold
- $J^P = \frac{1}{2}^-$ (experimentally unconfirmed)
- can only be observed by reconstructing $(\Sigma\pi)^0$ spectrum
- has always been a puzzle on what the nature of the state is
  - past experiments have found the lineshape (= invariant $\Sigma\pi$ mass distribution) to be distorted from a simple Breit-Wigner form
- what is the nature of this distorted lineshape?
  - "normal" qqq-baryon resonance
  - $L = 1$ SU(3) singlet in constituent quark model
  - molecular $N\overline{K}$ bound state
  - uds singlet coupled to S-wave meson-baryon systems
  - $udsg$ hybrid, $qqqq\overline{q}$
  - dynamically generated resonance in unitary coupled channel approach

unitary coupled channel approach

dynamically generate $\mathbf{\Lambda(1405)}$

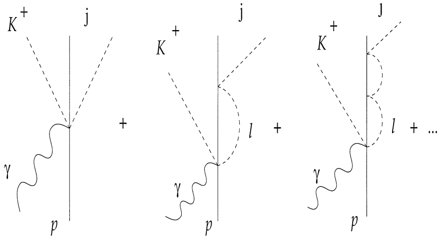

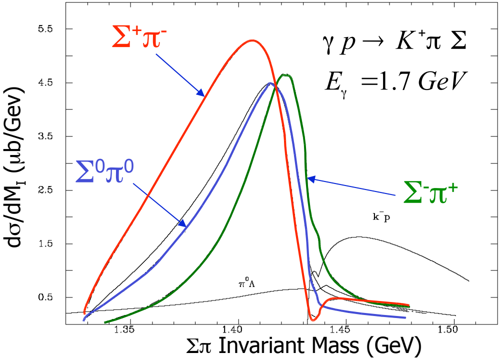

J. C. Nacher et al., Phys. Lett. B455, 55 (1999)

difference in lineshape

$$\frac{d\sigma(\pi^+\Sigma^-)}{dM_I} \propto \frac{1}{2}\left|T^{(1)}\right|^2 + \frac{1}{3}\left|T^{(0)}\right|^2 + \frac{2}{\sqrt{6}}\mathrm{Re}\left(T^{(0)}T^{(1)*}\right) + O\left(T^{(2)}\right)$$

$$\frac{d\sigma(\pi^-\Sigma^+)}{dM_I} \propto \frac{1}{2}\left|T^{(1)}\right|^2 + \frac{1}{3}\left|T^{(0)}\right|^2 - \frac{2}{\sqrt{6}}\mathrm{Re}\left(T^{(0)}T^{(1)*}\right) + O\left(T^{(2)}\right)$$

$$\frac{d\sigma(\pi^0\Sigma^0)}{dM_I} \propto \frac{1}{3}\left|T^{(0)}\right|^2 + O\left(T^{(2)}\right)$$

J. C. Nacher et al., Nucl. Phys. B455, 55

- difference in lineshapes is due to interference of isospin terms in calculation ($T^{(I)}$ represents amplitude of isospin I term)

goals of $\Lambda(1405)$ analysis

- measure the lineshape in the three $\Sigma\pi$ channels ($\Sigma^+\pi^-$, $\Sigma^0\pi^0$, $\Sigma^-\pi^+$)
- determine the differential cross section (what kind of angular/Mandelstam t dependence?)
- if distortion of lineshape is observed, this could be the first observation of a non-qqq baryonic structure
- determine the spin and parity

the g11a data set taken at CLAS

- ran from May to July 2004
- photoproduction experiment on a proton target
- photon energies from below $\Lambda(1405)$ threshold to 3.84 GeV
- large dataset with ~ 20 billion triggers
- current estimates of reconstructed $\Lambda(1405)$ events: ~ 272K (from fits shown later)

data is binned in:

- 10 bins of 100 MeV wide W bins
- ~ 20 bins of t in each W bin

reaction of interest

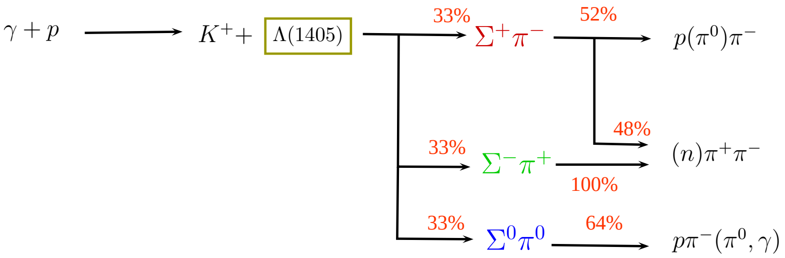

- $\mathbf{3}$ $\boldsymbol{\Sigma\pi}$ decay channels ($\mathbf{2}$ decay modes for $\boldsymbol{\Sigma^+\pi^-}$)
- This will be the first experimental result to compare all $\mathbf{3}$ $\boldsymbol{\Sigma\pi}$ decay modes

decay channel selection cut

example in 1 bin:

- $\gamma + \mathrm{p} \to K^+\pi^+\pi^-(n)$
- detect K^+, π^+, π^-, reconstruct missing neutron
- fit to Gaussian and select $\pm 3\sigma$ around neutron peak

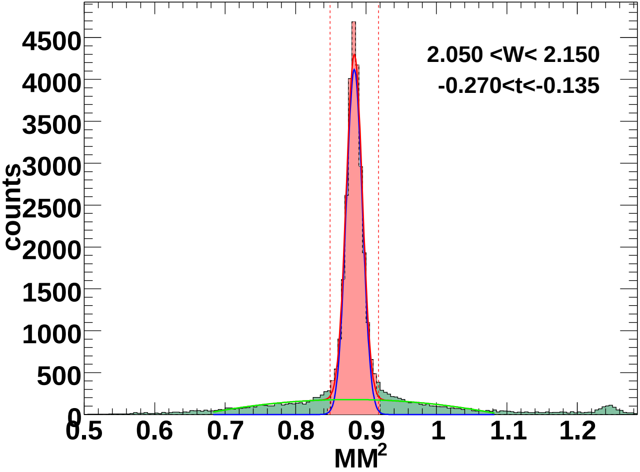

intermediate ground state hyperon

example in 1 bin:

- neutron combined with $\pi^\pm$ reconstructs $\Sigma^\pm$
- project on each axis, select $\pm 2\sigma$, exclude other hyperon
- diagonal band (K^0 from $\pi^+\pi^-$) is also excluded

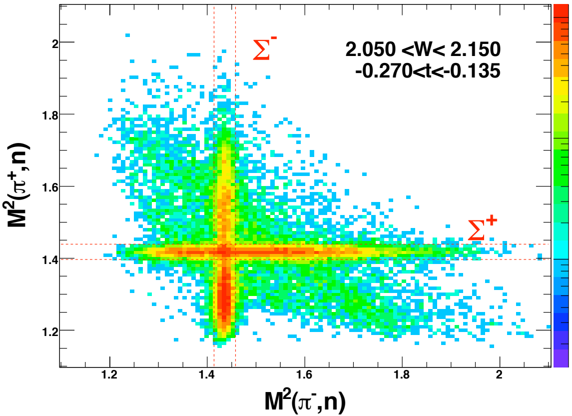

background (1) – $\Sigma(1385)$

- close in mass and width to $\Lambda(1405)$
- decays primarily to $\Lambda\pi^0$ (B.R. $\sim 88\%$)
- small B.R. to $\Sigma^\pm\pi^\mp$: $\sim 6\%$ each

$\Rightarrow$ calculate $\Sigma(1385)$ cross section in each bin from $\Lambda\pi^0$ channel, then scale down by B.R. to extract yield in $\Sigma\pi$ channels

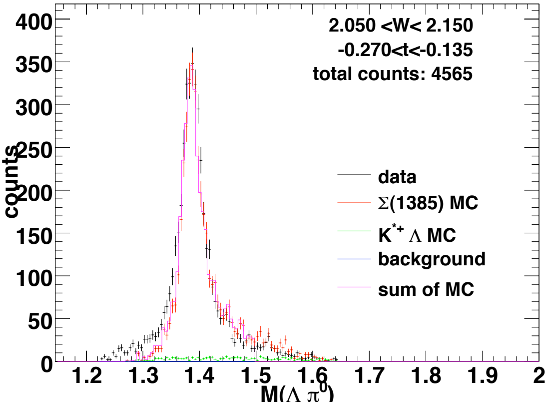

background (1) – $\Sigma(1385)$

- close in mass and width to $\Lambda(1405)$
- decays primarily to $\Lambda\pi^0$ (B.R. $\sim 88\%$)
- small B.R. to $\Sigma^{\pm}\pi^{\mp}$: $\sim 6\%$ each

$\Rightarrow$ calculate $\Sigma(1385)$ cross section in each bin from $\Lambda\pi^0$ channel, then scale down by B.R. to extract yield in $\Sigma\pi$ channels

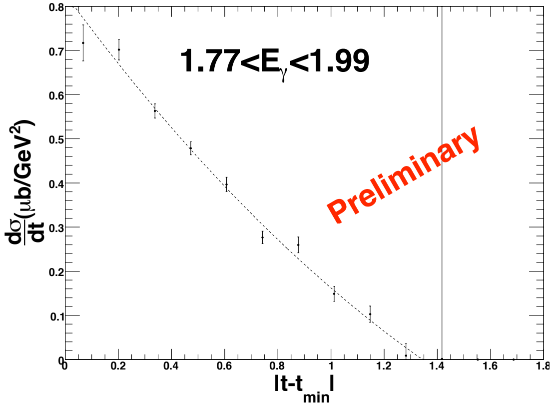

background (2) – $K^{*0}\Sigma^+$

- $\mathbf{\Gamma \sim 50}$ MeV
- strong overlap with $\mathbf{\Lambda(1405)}$ in lower $\boldsymbol{W}$ bins, separated at higher energies

$\Rightarrow$ generated MC and subtract off incoherently
(checks need to be done for interference)

low energy bin

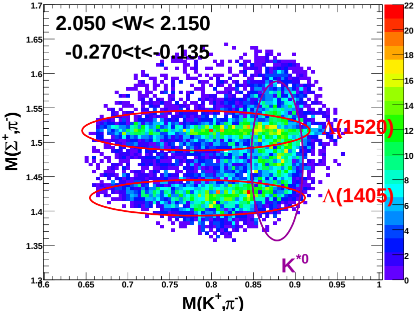

high energy bin

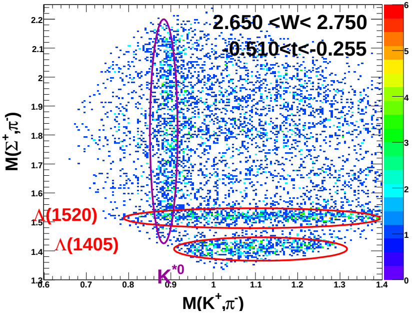

example of fit to lineshape

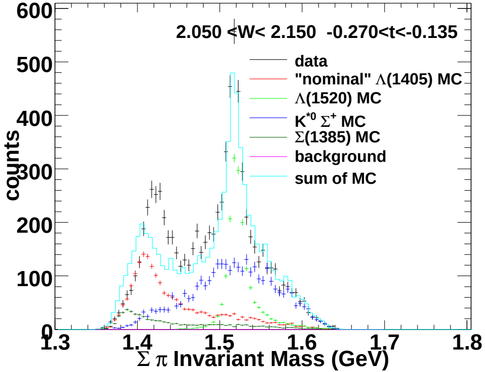

reaction:

$$\gamma + p \rightarrow K^+ + \boxed{\Lambda(1405)}$$
$$\rightarrow \boxed{\Sigma^+} + \pi^-$$
$$\rightarrow n + \pi^+$$

"nominal" $\Lambda(1405)$

- Monte Carlo generated with PDG values of mass, width
- all Monte Carlo was processed through detector simulation

example of fit to lineshape

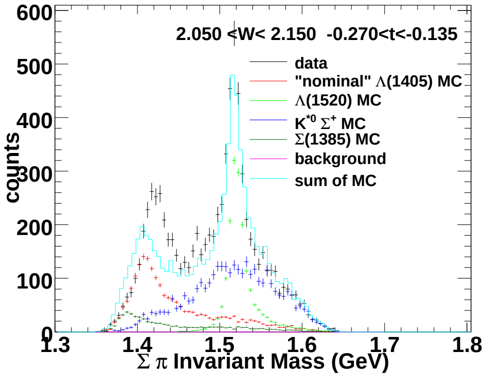

reaction:

$$\gamma + p \rightarrow K^+ + \boxed{\Lambda(1405)}$$
$$\rightarrow \boxed{\Sigma^+} + \pi^-$$
$$\rightarrow n + \pi^+$$

$\Sigma(1385)$

- strong overlap with $\Lambda(1405)$ due to close mass and width
- $\Lambda\pi^0$ decay mode was used to fix yield in $\Sigma\pi$ decay modes
- Monte Carlo generated with PDG values of mass, width

example of fit to lineshape

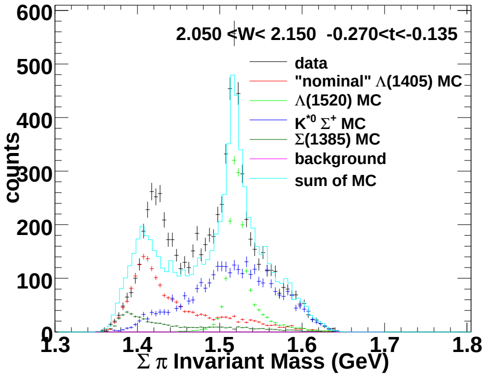

reaction:

$$\gamma + p \to K^+ + \boxed{\Lambda(1405)}$$
$$\to \boxed{\Sigma^+} + \pi^-$$
$$\to n + \pi^+$$

$\Lambda(1520)$

- Monte Carlo generated with PDG values of mass, width
- well-established Breit-Wigner lineshape

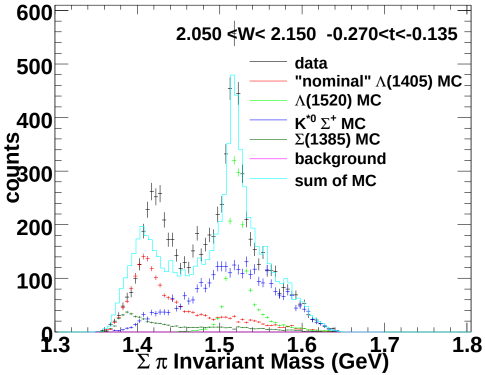

reaction:

$$\gamma + p \to K^+ + \boxed{\Lambda(1405)}$$
$$\to \boxed{\Sigma^+} + \pi^-$$
$$\to n + \pi^+$$

K^{*0}

- strong kinematic overlap with $\Lambda(1405)$
- Monte Carlo generated with PDG values of mass, width

example of fit to lineshape

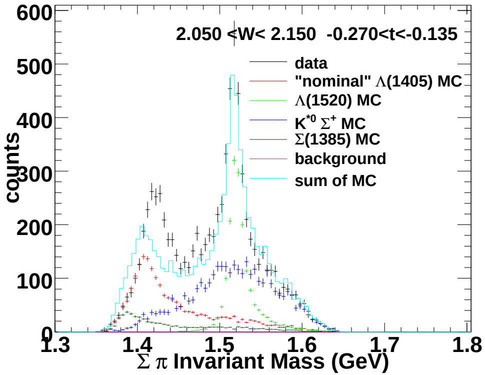

reaction:

$$\gamma + p \rightarrow K^{+} + \boxed{\Lambda(1405)}$$
$$\rightarrow \boxed{\Sigma^{+}} + \pi^{-}$$
$$\rightarrow n + \pi^{+}$$

$\Rightarrow$ after fitting with the above templates, we subtracted off contributions from the $\Sigma(1385)$, $\Lambda(1520)$, K^{*0}, and assigned the remaining contribution to the $\Lambda(1405)$.

acceptance correction

- after subtracting background contributions, we are left with "residual" spectrum
- to correct for dependence of the lineshape on acceptance, we have calculated the acceptance as a function of lineshape
- our lineshape results are summed over the t bins in each energy bin

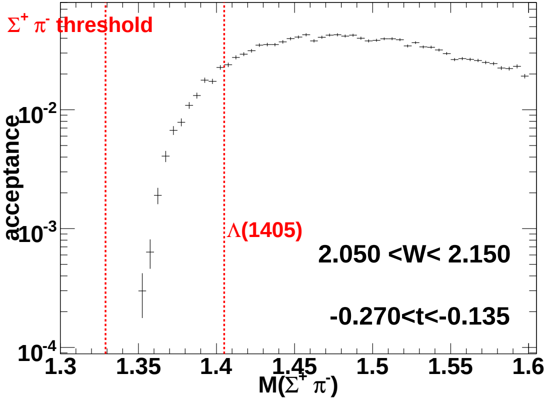

results of lineshape after acceptance correction

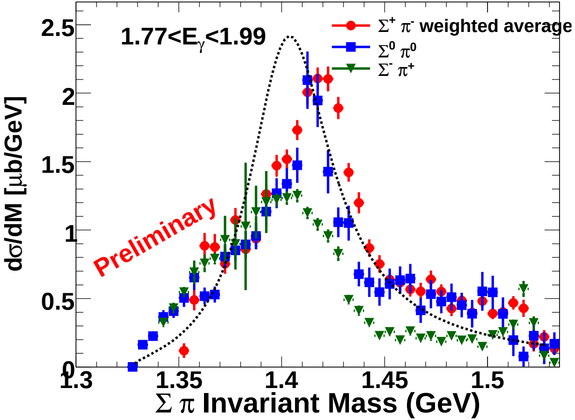

different lineshapes for each $\Sigma\pi$ decay mode

- lineshapes do appear different for each $\Sigma\pi$ decay mode
- $\Sigma^+\pi^-$ decay mode has peak at highest mass, most narrow

results of lineshape after acceptance correction

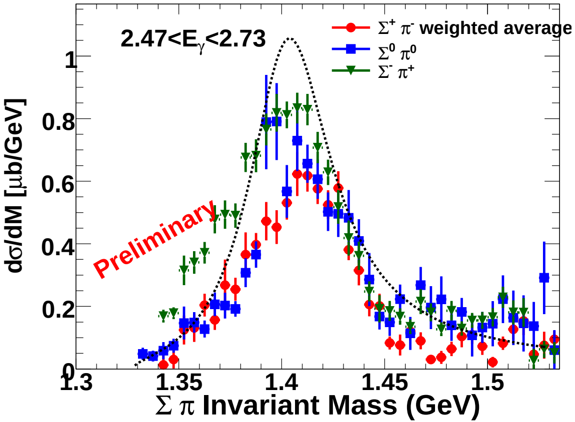

different lineshapes for each $\Sigma\pi$ decay mode

- lineshapes do appear different for each $\Sigma\pi$ decay mode
- $\Sigma^+\pi^-$ decay mode has peak at highest mass, most narrow

results of lineshape after acceptance correction

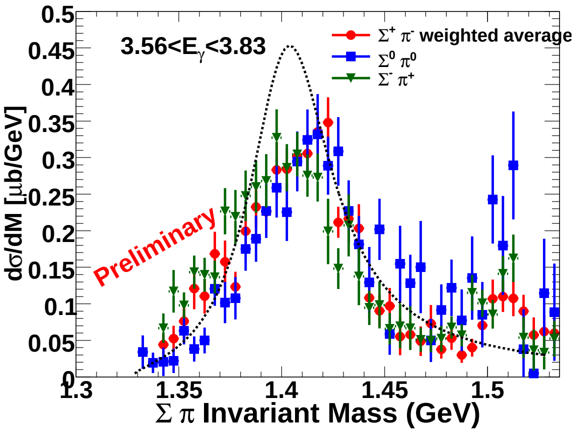

different lineshapes for each $\Sigma\pi$ decay mode

- lineshapes do appear different for each $\Sigma\pi$ decay mode
- $\Sigma^+\pi^-$ decay mode has peak at highest mass, most narrow

theory prediction from chiral unitary approach

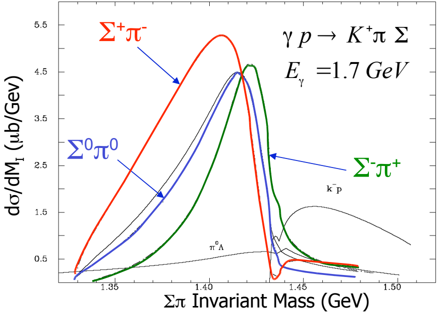

J. C. Nacher et al., Nucl. Phys. B455, 55

$$\frac{d\sigma(\pi^+\Sigma^-)}{dM_I} \propto \frac{1}{2}\left|T^{(1)}\right|^2 + \frac{1}{3}\left|T^{(0)}\right|^2 + \frac{2}{\sqrt{6}}\mathrm{Re}\left(T^{(0)}T^{(1)*}\right) + O\left(T^{(2)}\right)$$

$$\frac{d\sigma(\pi^-\Sigma^+)}{dM_I} \propto \frac{1}{2}\left|T^{(1)}\right|^2 + \frac{1}{3}\left|T^{(0)}\right|^2 - \frac{2}{\sqrt{6}}\mathrm{Re}\left(T^{(0)}T^{(1)*}\right) + O\left(T^{(2)}\right)$$

$$\frac{d\sigma(\pi^0\Sigma^0)}{dM_I} \propto \frac{1}{3}\left|T^{(0)}\right|^2 + O\left(T^{(2)}\right)$$

- $\Sigma^-\pi^+$ decay mode peaks at highest mass, most narrow
- difference in lineshapes is due to interference of isospin terms in calculation ($\boldsymbol{T^{(I)}}$ represents amplitude of isospin $\boldsymbol{I}$ term)

differential cross sections

- summing over the lineshape gives differential cross section
- $\mathbf{\Lambda(1520)}$ serves as a check of systematics
- at lower energies where lineshapes differ, differences in $\frac{d\sigma}{dt}$ are observed

$$\frac{d\sigma}{dt}[\mu b/\mathrm{GeV}^2] \text{ for } 2.050 < W < 2.150 \text{ (GeV)}$$

$\Lambda(1405)$

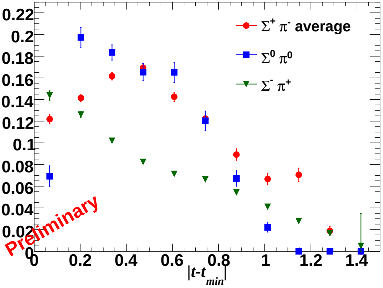

$\Lambda(1520)$

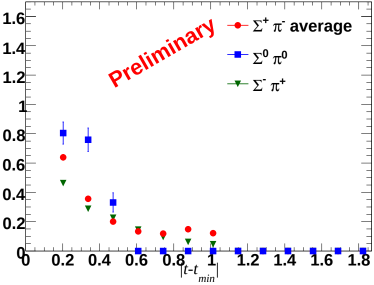

differential cross sections

- summing over the lineshape gives differential cross section
- $\mathbf{\Lambda(1520)}$ serves as a check of systematics
- at lower energies where lineshapes differ, differences in $\frac{\mathbf{d}\boldsymbol{\sigma}}{\mathbf{d}\boldsymbol{t}}$ are observed

$$\frac{\mathbf{d}\boldsymbol{\sigma}}{\mathbf{d}\boldsymbol{t}}[\boldsymbol{\mu b}/\mathbf{GeV^2}] \text{ for } \mathbf{2.350} < \boldsymbol{W} < \mathbf{2.450} \text{ (GeV)}$$

$\mathbf{\Lambda(1405)}$

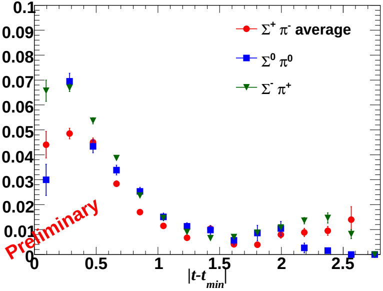

$\mathbf{\Lambda(1520)}$

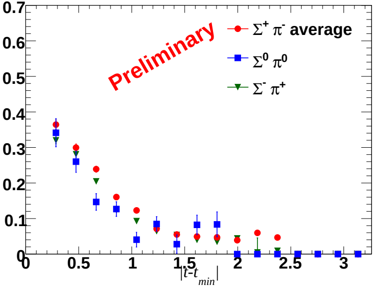

differential cross sections

- summing over the lineshape gives differential cross section
- $\mathbf{\Lambda(1520)}$ serves as a check of systematics
- at lower energies where lineshapes differ, differences in $\frac{d\sigma}{dt}$ are observed

$$\frac{d\sigma}{dt}[\mu b/\mathrm{GeV}^2] \text{ for } 2.750 < W < 2.840 \text{ (GeV)}$$

$\Lambda(1405)$

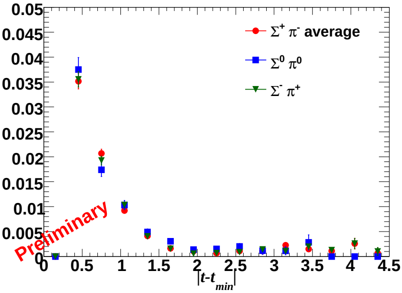

$\Lambda(1520)$

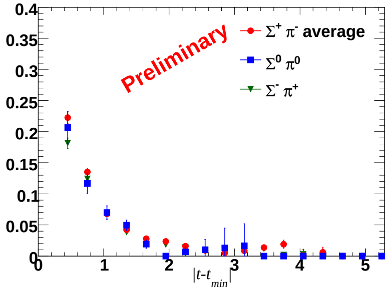

J^P of $\Lambda(1405)$

no previous **direct experimental evidence** for the spin and parity of the $\Lambda(1405)$ (PDG assumes $1/2^-$)

How do we measure these quantities?

- **spin** – measure distribution into $\Sigma\pi$
  - flat distribution is best evidence possible for $J = 1/2$
- **parity** – measure polarization of Σ from $\Lambda(1405)$
  - Polarization direction as a function of Σ decay angle will be determined by J^P of $\Lambda(1405)$

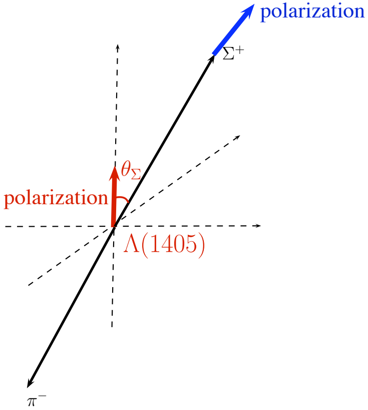

s-wave, p-wave scenario

$\underline{L = 0}$ (s-wave)

$$\vec{P}_{\Sigma^+} = \vec{P}_{\Lambda^*}$$

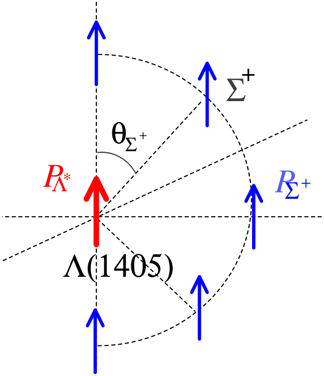

$\Lambda(1405) \longrightarrow \Sigma\pi$ is s-wave

$$\Leftrightarrow J^P = 1/2^-$$

$\underline{L = 1}$ (p-wave)

$$\vec{P}_{\Sigma^+} = |\vec{P}_{\Lambda^*}|\hat{n}(2\theta_{\Sigma^+})$$

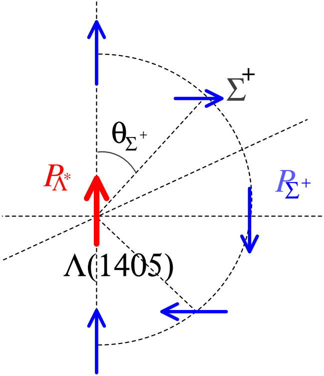

$\Lambda(1405) \longrightarrow \Sigma\pi$ is p-wave

$$\Leftrightarrow J^P = 1/2^+$$

determination of spin of $\Lambda(1405)$

fits to $J = \frac{1}{2}$ and $J = \frac{3}{2}$ distributions done to

- $\Lambda(1405) \rightarrow \Sigma^+\pi^-$
- $\Sigma(1385) \rightarrow \Lambda\pi^0$
- 3 bins of W centered at $2.6, 2.7, 2.8$ GeV with forward K^+angles
- selected region has kinematic separation from K^{*0} bg

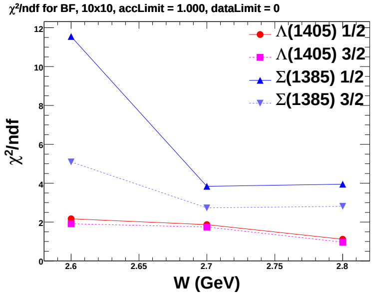

with $J = 3/2$ fit, χ^2/ndf is reduced for $\Sigma(1385)$, but almost no reduction for $\Lambda(1405)$

determination of spin of $\Lambda(1405)$

fits to $J = \frac{1}{2}$ and $J = \frac{3}{2}$ distributions done to

- $\Lambda(1405) \rightarrow \Sigma^+\pi^-$
- $\Sigma(1385) \rightarrow \Lambda\pi^0$
- 3 bins of W centered at $2.6, 2.7, 2.8$ GeV with forward K^+angles
- selected region has kinematic separation from K^{*0} bg

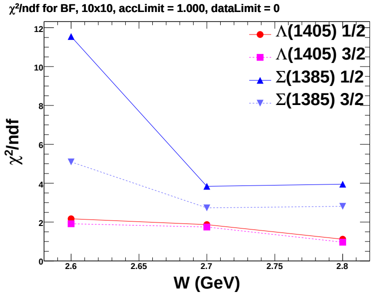

with $J = 3/2$ fit, χ^2/ndf is reduced for $\Sigma(1385)$, but almost no reduction for $\Lambda(1405)$

$\Rightarrow$ best possible evidence for $J = 1/2$

determination of parity

polarization of $\Lambda(1405)$ in direction $\perp$ to production plane is measured

- $W = 2.6$ GeV
- forward K^+angles
- use reaction: $\Lambda(1405) \to \Sigma^+\pi^-$, $\Sigma^+ \to p\pi^0$
- very large hyperon decay parameter $\alpha = -0.98$

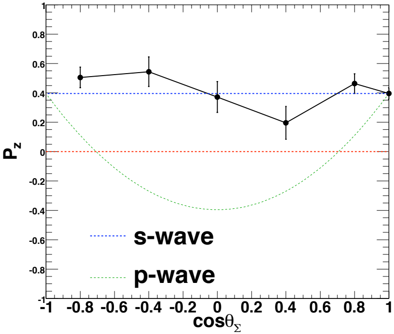

determination of parity

polarization of $\Lambda(1405)$ in direction $\perp$ to production plane is measured

- $W = 2.6$ GeV
- forward K^+angles
- use reaction: $\Lambda(1405) \to \Sigma^+\pi^-$, $\Sigma^+ \to p\pi^0$
- very large hyperon decay parameter $\alpha = -0.98$

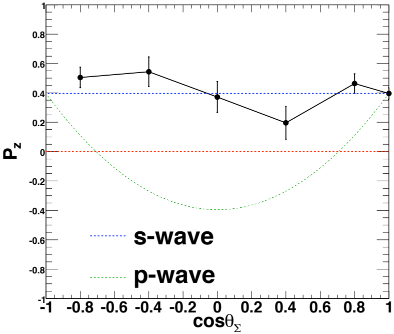

polarization does not change with Σ^+ angle (θ_{Σ^+})

determination of parity

polarization of $\Lambda(1405)$ in direction $\perp$ to production plane is measured

- $W = 2.6$ GeV
- forward K^+angles
- use reaction: $\Lambda(1405) \to \Sigma^+\pi^-$, $\Sigma^+ \to p\pi^0$
- very large hyperon decay parameter $\alpha = -0.98$

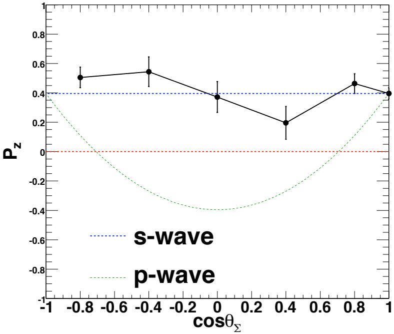

polarization does not change with Σ^+ angle (θ_{Σ^+})

$\Rightarrow$ $J^P = 1/2^-$ is confirmed

determination of parity

polarization of $\Lambda(1405)$ in direction $\perp$ to production plane is measured

- $W = 2.6$ GeV
- forward K^+angles
- use reaction:
  $\Lambda(1405) \rightarrow \Sigma^+\pi^-$,
  $\Sigma^+ \rightarrow p\pi^0$
- very large hyperon decay parameter $\alpha = -0.98$

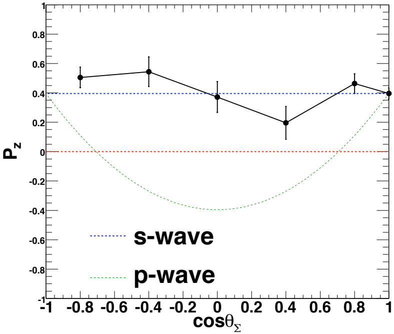

polarization does not change with Σ^+ angle (θ_{Σ^+})

$\Rightarrow J^P = 1/2^-$ is confirmed

furthermore, this measured Σ^+ polarization **is** the $\Lambda(1405)$ polarization

determination of parity

polarization of $\Lambda(1405)$ in direction $\perp$ to production plane is measured

- $W = 2.6$ GeV
- forward K^+angles
- use reaction:
  $\Lambda(1405) \rightarrow \Sigma^+\pi^-$,
  $\Sigma^+ \rightarrow p\pi^0$
- very large hyperon decay parameter $\alpha = -0.98$

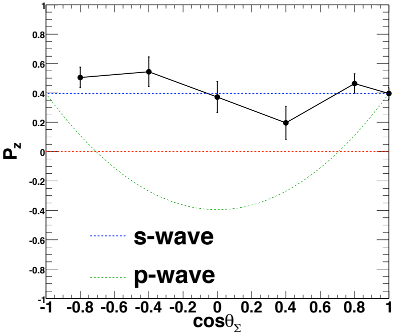

polarization does not change with Σ^+ angle (θ_{Σ^+})

$\Rightarrow J^P = 1/2^-$ is confirmed

furthermore, this measured Σ^+ polarization **is** the $\Lambda(1405)$ polarization

$\Rightarrow \Lambda(1405)$ is produced with $\sim 40\%$ polarization

conclusion

- high statistics measurement of $\mathbf{\Lambda(1405)}$ photoproduction has been done with CLAS at Jlab
- **difference in lineshape for different decay modes** has been observed
- **difference in cross section for different decay modes** has been observed
- **spin and parity are experimentally established for the first time**
- as a bonus, **polarization of $\Lambda(1405)$ is found to be $\sim 40\%$ at $\boldsymbol{W \sim 2.6}$ GeV, forward K^+angles**

$\Rightarrow$ best evidence to date of possible deviation from a simple $\boldsymbol{qqq}$-structure.